Ang-2/VEGF bispecific antibody reprograms macrophages and resident microglia to anti-tumor phenotype and prolongs glioblastoma survival

Jonas Kloepper[a,1], Lars Riedemann[a,1,2,3], Zohreh Amoozgar[a,1], Giorgio Seano[a], Katharina Susek[a], Veronica Yu[a], Nisha Dalvie[a], Robin L. Amelung[a], Meenal Datta[a,b], Jonathan W. Song[a,4], Vasileios Askoxylakis[a], Jennie W. Taylor[a,c,5], Christine Lu-Emerson[a,c,6], Ana Batista[a,7], Nathaniel D. Kirkpatrick[a,8], Keehoon Jung[a], Matija Snuderl[a,d,9], Alona Muzikansky[e], Kay G. Stubenrauch[f], Oliver Krieter[f], Hiroaki Wakimoto[g], Lei Xu[1], Lance L. Munn[a], Dan G. Duda[a], Dai Fukumura[a], Tracy T. Batchelor[c,10], and Rakesh K. Jain[a,10]

[a]Edwin L. Steele Laboratories, Department of Radiation Oncology, Massachusetts General Hospital and Harvard Medical School, Boston, MA 02114; [b]Department of Chemical and Biological Engineering, Tufts University, Medford, MA 02155; [c]Stephen E. and Catherine Pappas Center for Neuro-Oncology, Department of Neurology, Massachusetts General Hospital and Harvard Medical School, Boston, MA 02114; [d]Department of Pathology, Massachusetts General Hospital and Harvard Medical School, Boston, MA 02114; [e]Biostatistics Center, Massachusetts General Hospital and Harvard Medical School, Boston, MA 02114; [f]Roche Pharma Research and Early Development, Roche Innovation Center Munich, 82377 Penzberg, Germany; and [g]Department of Neurosurgery, Massachusetts General Hospital and Harvard Medical School, Boston, MA 02114

Contributed by Rakesh K. Jain, December 28, 2015 (sent for review December 1, 2015; reviewed by James W. Hodge and Balveen Kaur)

Inhibition of the vascular endothelial growth factor (VEGF) pathway has failed to improve overall survival of patients with glioblastoma (GBM). We previously showed that angiopoietin-2 (Ang-2) overexpression compromised the benefit from anti-VEGF therapy in a preclinical GBM model. Here we investigated whether dual Ang-2/VEGF inhibition could overcome resistance to anti-VEGF treatment. We treated mice bearing orthotopic syngeneic (Gl261) GBMs or human (MGG8) GBM xenografts with antibodies inhibiting VEGF (B20), or Ang-2/VEGF (CrossMab, A2V). We examined the effects of treatment on the tumor vasculature, immune cell populations, tumor growth, and survival in both the Gl261 and MGG8 tumor models. We found that in the Gl261 model, which displays a highly abnormal tumor vasculature, A2V decreased vessel density, delayed tumor growth, and prolonged survival compared with B20. In the MGG8 model, which displays a low degree of vessel abnormality, A2V induced no significant changes in the tumor vasculature but still prolonged survival. In both the Gl261 and MGG8 models A2V reprogrammed protumor M2 macrophages toward the antitumor M1 phenotype. Our findings indicate that A2V may prolong survival in mice with GBM by reprogramming the tumor immune microenvironment and delaying tumor growth.

anti-angiogenic therapy | tumor microenvironment | anti-tumor immunity | macrophage polarization | microglia reprogramming

Significance

Improving survival of patients with glioblastoma (GBM) using antiangiogenic therapy remains a challenge. In this study we show that dual blockade of angiopoietin-2 and vascular endothelial growth factor delays tumor growth and enhances survival benefits through reprogramming of tumor-associated macrophages toward an antitumor phenotype as well as by pruning immature tumor vessels. The antitumor immunomodulatory potential of this dual blockade supports clinical testing of this approach for GBM with other immunotherapeutic approaches such as checkpoint blockers.

Glioblastoma (GBM) is the most common primary malignant brain tumor in adults. Even after maximal safe resection and chemoradiation, most patients survive little more than 1 y (1, 2). Bevacizumab, a humanized monoclonal antibody against vascular endothelial growth factor (VEGF), was conditionally approved in 2009 in the United States for treatment of recurrent GBM (rGBM) (2–5). Adding bevacizumab to the standard regimen of radiotherapy and alkylating chemotherapy with temozolomide confers an increase in progression-free survival (PFS) but does not improve overall survival in newly diagnosed GBM (nGBM) patients (6, 7). Similarly, cediranib, an oral pan-VEGF receptor tyrosine kinase inhibitor, fails to improve overall survival in patients with rGBM (8). Most recently a European Organization for the Research and Treatment of Cancer randomized phase III trial (EORTC 26101) showed that bevacizumab plus lomustine does not improve survival in patients with progressive GBM, although it prolongs progression-free survival (9). We previously have shown that angiopoietin-2 (Ang-2) is a resistance pathway to anti-VEGF therapy in a preclinical model of GBM (10). Ang-2 competes with angiopoietin-1 (Ang-1) in binding to the TEK receptor tyrosine kinase (Tie-2) receptor (11, 12). In physiological settings, Ang-1 activates Tie-2 and stabilizes blood vessels, whereas Ang-2 inhibits

Author contributions: J.K., L.R., Z.A., G.S., V.Y., N.D., R.L.A., J.W.S., V.A., A.B., N.D.K., M.S., K.G.S., O.K., H.W., L.X., L.L.M., D.G.D., D.F., T.T.B., and R.K.J. designed research; J.K., L.R., Z.A., K.S., V.Y., N.D., R.L.A., M.D., J.W.S., J.W.T., and C.L.-E. performed research; J.K., L.R., Z.A., G.S., K.S., V.Y., N.D., R.L.A., M.D., J.W.S., J.W.T., C.L.-E., A.B., K.J., and A.M. analyzed data; and J.K., L.R., Z.A., G.S., M.D., J.W.S., L.X., D.G.D., D.F., T.T.B., and R.K.J. wrote the paper.

Reviewers: J.W.H., Center for Cancer Research, National Cancer Institute; and B.K., Comprehensive Cancer Center, The Ohio State University.

Conflict of interest statement: R.K.J. received consultant fees from Ophthotech, SPARC, SynDevRx, and XTuit. R.K.J. owns equity in Enlight, Ophthotech, SynDevRx, and XTuit and serves on the Board of Directors of XTuit and on the Boards of Trustees of Tekla Healthcare Investors, Tekla Life Sciences Investors, Tekla Healthcare Opportunities Fund, and Tekla World Healthcare Fund. No reagents or funding from these companies was used in these studies. T.T.B. received consultant fees from Merck, Roche, Kirin Pharmaceuticals, Spectrum Pharmaceuticals, Novartis, and Champions Biotechnology. K.G.S. and O.K. are employees of Roche.

Freely available online through the PNAS open access option.

[1]J.K., L.R., and Z.A. contributed equally to this work.

[2]Present address: Neurology Clinic and National Center for Tumor Diseases, University Hospital Heidelberg, 69120 Heidelberg, Germany.

[3]Present address: Clinical Cooperation Unit Neuro-Oncology, German Cancer Consortium, German Cancer Research Center, 69120 Heidelberg, Germany.

[4]Present address: Department of Mechanical and Aerospace Engineering, Ohio State University, Columbus, OH 43210.

[5]Present address: Department of Neurological Surgery, University of California, San Francisco, CA 94143.

[6]Present address: Department of Neurology, Maine Medical Center, Portland, ME 04102.

[7]Present address: Cell Press, Trends in Cancer, Cambridge, MA 02139.

[8]Present address: Novartis Institutes for BioMedical Research Inc., Cambridge, MA 02139.

[9]Present address: Department of Pathology, New York University Langone Medical Center and Medical School, New York, NY 10016.

[10]To whom correspondence may be addressed. Email: tbatchelor@mgh.harvard.edu or jain@steele.mgh.harvard.edu.

This article contains supporting information online at www.pnas.org/lookup/suppl/doi:10.1073/pnas.1525360113/-/DCSupplemental.

www.pnas.org/cgi/doi/10.1073/pnas.1525360113

Tie-2 signaling, destabilizes blood vessels, and facilitates VEGF-induced angiogenesis in a context-dependent manner (13). In tumors, however, Ang-2 may act as a partial Tie-2 agonist, conferring therapy resistance by protecting endothelial cells (EC) from therapeutic VEGF withdrawal (14). The tumor growth-supportive role of Ang-2 in GBMs is not confined to the vascular compartment. Ang-2 also has been shown to mediate the homing of Tie-2^{+} macrophages to human GBMs (15, 16). In the tumor microenvironment, the macrophage population then is reprogrammed to a protumor (17–19), proangiogenic phenotype (20–22) in an Ang-2–dependent manner (22). Tumor-associated macrophages (TAMs) have a broad phenotypic spectrum, and their polarization can change in response to their microenvironment. The two extremes of the phenotypic spectrum of TAMs are defined as the alternatively activated protumor (M2) versus classically activated antitumor (M1) states (23–25). We previously have shown that the degree of TAM infiltration in GBM patients treated with anti-VEGF therapy is inversely correlated with survival (26). These data point to the role of TAMs as potential mediators of resistance to anti-VEGF therapy in GBM. Here we used a dual Ang-2/VEGF-inhibiting antibody (A2V) in orthotopic syngeneic (Gl261 graft) and patient-derived cell line (MGG8 xenograft) models of GBM. We show that A2V treatment can reprogram TAMs to the antitumor M1 state. Moreover, we further dissect the reprogramming effects in the overall TAM population and show that both recruited macrophages and resident microglia can be therapeutically altered by dual Ang-2/VEGF inhibition. Combined anti–Ang-2/VEGF therapy was shown to delay tumor growth and prolong survival in a number of extracranial tumor models (27–30). Although anti–Ang-2/VEGF therapy is being tested in GBM patients (NCT01609790, NCT01248949, NCT01290263) and in other solid malignancies (Table S1). The bispecific antibody A2V has been shown to be safe in a first-in-human study (NCT01688206) in patients with locally advanced or metastatic solid tumors (31). Here we show that the murinized Ang-2/VEGF–neutralizing antibody A2V (CrossMab) is effective in two different GBM models and delays tumor growth through vascular and/or immunomodulatory effects.

Results

Ang-2/VEGF Inhibition Delays Tumor Growth and Prolongs Survival. We first validated Ang-2 as a potential target in GBM patients by analyzing publicly available data portals, i.e., The Cancer Genome Atlas (TCGA) and Gene Expression Omnibus (32–34). We found that Ang-2 is expressed in newly diagnosed GBM [nGBM] and rGBM (Fig. S1*A*) across molecular subtypes (Fig. S1*B*), significantly correlates with VEGF expression (Fig. S1*E*), and is predominantly expressed in GBM blood vessels in patients (Fig. S1 *C* and *D*). Next we investigated the effects of blocking Ang-2 and VEGF alone or in combination with Ang-2 in an orthotopic syngeneic murine GBM model (Gl261 in C57BL/6 mice). The Gl261 model recapitulates abnormal GBM tumor vessels and the presence of intratumoral foci of necrosis and displays a moderate degree of invasion into the surrounding brain. We treated Gl261-bearing animals with IgG control or with antibodies inhibiting Ang-2 (LC06), VEGF (B20), or Ang-2/VEGF (A2V) and found that all experimental therapies increased survival compared with IgG control (Fig. 1*A*). In addition, we found that A2V treatment significantly extended median survival compared with either LC06 or B20 alone (Fig. 1*A*). Next we tested if the effects we observed in the Gl261 model were conserved in the MGG8 model. The MGG8 model is characterized by extensive single-cell invasion but a tumor vasculature that is less abnormal than seen with Gl261. In the MGG8 model, both LC06 and B20 failed to confer a survival benefit compared with IgG, but A2V prolonged survival compared with all treatment groups (Fig. 1*B*). To assess the antiangiogenic potential of LC06, B20, and A2V, we next measured the effects of these antibodies on primary ECs (human umbilical vein ECs, HUVECs) in a microfluidic chamber assay (Fig. S2). We found that the combination

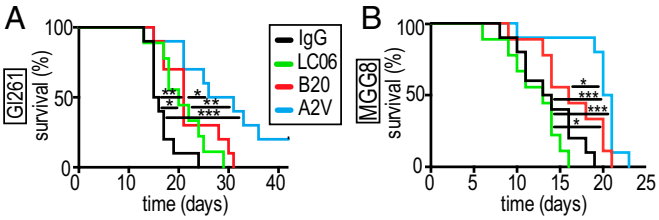

Fig. 1. Treatment with A2V prolongs survival and delays tumor growth in the orthotopic Gl261 and the MGG8 models. (*A*) In the Gl261 model, treatment with A2V ($n = 10$) led to a survival benefit compared with IgG [hazard ratio (HR) 3.93, 95% confidence interval (CI) 4.15–35.97, $***P = < 0.001$, $n = 10$], LC06 (HR 2.99, 95% CI 1.6–13.49, $**P = 0.0098$, $n = 9$), and B20 (HR 2.35, 95% CI, 1.31–9.12, $*P = 0.03$, $n = 10$) treatment. LC06 prolonged survival compared with IgG treatment (HR 2.32, 95% CI 1.31–8.98, $*P = 0.03$, $n = 9$), and B20 increased survival compared with IgG treatment (HR 2.68, 95% CI 2.03–14.58, $**P = 0.005$, $n = 10$). (*B*) In the MGG8 model treatment with LC06 ($n = 9$) or B20 ($n = 9$) did not prolong survival compared with IgG treatment ($n = 10$). Therapy with B20 significantly prolonged survival compared with LC06 therapy (HR 2.48, 95% CI 1.47–11.31, $*P = 0.02$, $n = 9$). Therapy with A2V ($n = 10$) prolonged survival compared with IgG (HR 3.83, 95% CI 4.07–35.39, $***P < 0.001$), LC06 (HR 4.14, 95% CI 4.76–49.81, $****P = < 0.001$, $n = 9$), and B20 (HR 2.28, 95% CI 1.51–11.13, $*P = 0.03$, $n = 9$) therapy. Time represents days post treatment initiation. Animals were treated once weekly i.p. with 10 mg/kg of IgG control, B20, LC06, or A2V.

of recombinant VEGF (rVEGF) plus recombinant Ang-2 (rAng-2) strongly induced sprouting in HUVECs. HUVEC sprouting induced by exogenous rVEGF alone was significantly inhibited by B20 but not by LC06 (Fig. S2 *A*–*F*). HUVEC sprouting induced by rVEGF plus rAng-2 (Fig. S2*J*) also was significantly inhibited by B20 (Fig. S2 *K* and *L*) but was not decreased by LC06 and was completely abrogated by A2V (Fig. S2*M*). Importantly, exogenous rAng2-induced EC sprouting was completely abolished not only by LC06 but also by B20 in the absence of exogenous rVEGF (Fig. S2 *G*–*I*). The angiogenic effect of Ang-2 appears to be dependent on VEGF signaling, which may contribute to the context-dependent functions of Ang-2. Based on these data and our observation that LC06 did not confer a survival benefit in the MGG8 model, we determined that Ang-2 blockade requires additional VEGF inhibition to inhibit angiogenesis effectively. Therefore we focused all further analyses on B20 and A2V compared with control.

In additional animal experiments we harvested GBM specimens for histological analyses in a time-matched fashion at a time point when viable tumor burden—as a surrogate of viable tumor burden (Fig. S3 *A* and *D*)—was significantly different from control: Gl261 tumors were harvested on day 5, and MGG8 tumors at day 10 after treatment initiation. To determine if antiangiogenic treatments with B20 and A2V decrease tumor burden, we monitored blood Gaussia luciferase (Gluc) activity (35–37) daily in Gl261-GFP-Gluc–bearing mice treated with IgG, B20, or A2V. Reduced blood Gluc activity in A2V-treated animals suggested lower tumor burden as compared with IgG or B20 treatment (Fig. S3*B*). Moreover, using the 5-ethynyl-2′-deoxyuridine (EdU) incorporation assay, we found that Gl261 tumors of A2V-treated animals exhibited reduced proliferation compared with IgG control or B20 therapy (Fig. S3*C*).

In the MGG8 model, levels of blood Gluc activity were lower in B20- and A2V-treated animals than in animals treated with IgG, suggesting therapy-induced reduction of viable tumor burden (Fig. S3*E*). Comparisons in the kinetics of tumor burden between B20- and A2V-treated MGG8-bearing animals failed to reach significance (Gluc assay). However, we measured significantly reduced tumor proliferation (EdU assay) in A2V- compared with B20-treated tumors (Fig. S3*F*). We detected no significant difference in apoptosis between the treatment groups in either Gl261 or MGG8 tumors (Fig. S4 *A* and *B*). Further in vitro experiments showed that neither B20 nor A2V had a direct effect on GBM cell viability in these models (Fig. S4 *C* and *D*), as is consistent with the absence of Tie-2 expression on the tumor cells (Fig. S4 *E* and *F*). Taken together our results demonstrate that A2V prolongs the survival of

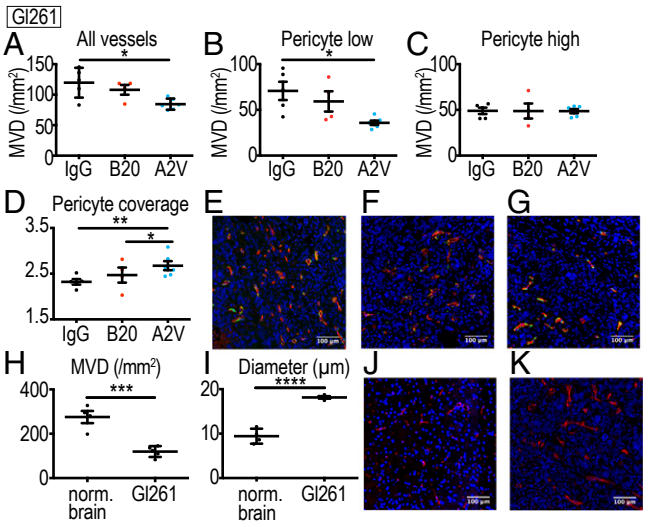

Fig. 2. A2V decreases tumor vessel density in Gl261 tumors. (*A*) A2V ($n = 6$) reduces total MVD (vessels/mm^2) compared with IgG (*$P = 0.01$, $n = 5$). (*B*) A2V treatment ($n = 6$) reduces MVD of blood vessels with low pericyte coverage compared with IgG treatment (*$P = 0.02$, $n = 5$). (*C*) No difference in the MVD of vessels with high pericyte coverage was detectable between treatment groups (IgG, $n = 6$; B20, $n = 6$; A2V, $n = 4$). (*D*) Pericyte coverage in pericyte-high vessels was higher with A2V ($n = 6$) compared to treatment with B20 (*$P = 0.03$) and IgG (**$P = 0.001$, $n = 5$). (*E–G*) Representative immunofluorescence images of IgG-, B20-, and A2V-treated tumors. Shown are tumor vessels (red), pericytes (green), and DAPI-stained nuclei (blue). (*H*) IgG-treated Gl261 tumors (day 5 post treatment initiation, $n = 5$) display lower MVD than seen in the normal brain (nl brain) of 10-wk-old C57BL/6 mice (***$P < 0.001$, $n = 4$). (*I*) The mean vessel diameter in IgG-treated Gl261 tumors ($n = 4$) is larger than that in normal C57BL/6 brain vessels (****$P < 0.0001$, $n = 4$). (*J* and *K*) Gl261 vessels are inhomogeneously distributed, dilated, and irregularly shaped as compared with normal brain vessels of C57BL/6 mice. Shown are representative immunofluorescence images of the normal brain (*J*) and Gl261 tumor vessels (*K*) stained for CD31 (red). MVD represents vessels/mm^2 tumor area; pericyte coverage represents desmin-positive pixels per vessel perimeter (pixels). (Scale bars, 100 µm.)

mice bearing Gl261 and MGG8 tumors by reducing in vivo tumor burden.

A2V Enhances Vessel Pruning as Compared with VEGF Inhibition Alone in the Gl261 Model. To determine if vessel-modulating effects are responsible for the prolonged survival and reduced tumor burden in the A2V group, we studied the effects of A2V on Gl261 tumor vessels (Fig. 2 *A–G*). The vasculature of Gl261 tumors is characterized by lower microvessel density (MVD) (Fig. 2*H*) and larger vessel diameters (Fig. 2*I*) than seen in the vasculature of the normal brain (Fig. 2 *H–K*). Using immunohistochemistry in Gl261 tumor tissues, we found that A2V-treated tumors displayed a lower MVD than IgG-treated tumors at day 5 after treatment initiation (Fig. 2*A*). Perivascular cells stabilize tumor vessels and can confer resistance to antiangiogenic treatment (38, 39). We found that the MVD of immature vessels with low pericyte coverage was significantly decreased (Fig. 2*B*). In contrast, the MVD of mature vessels with high pericyte coverage was similar across treatment groups (Fig. 2*C*). Interestingly, A2V treatment in the Gl261 model further increased pericyte coverage of the remaining pericyte-high vessels, as compared with IgG and B20 treatments (Fig. 2 *D–G*). Collectively, our experiments show that in Gl261 tumors more potent antiangiogenic effects on immature pericyte-low vessels are seen with A2V treatment than with B20 treatment.

A2V Reduces Tumor Burden in the MGG8 Model Without Vessel Pruning. Next, we tested if the vascular effects observed in the Gl261 model (Fig. 2 *A–G*) could also be observed in the MGG8 model (Fig. 3 *A–H*). The MGG8 vasculature showed a lower degree of abnormality, with vessel architecture resembling the normal mouse brain (Fig. 3 *H–K*). MGG8 tumors have a higher MVD than the Gl261 model (Fig. 3*H*), and vessels are homogeneously distributed, less tortuous, and smaller in diameter (Fig. 3 *I–K*). Immunohistochemical analyses showed that, in contrast to the Gl261 model, A2V treatment induced no significant changes in MVD or pericyte coverage compared with B20- or IgG-treated MGG8 tumors (Fig. 3 *A–D*). These results indicate that the reduction of tumor burden after A2V treatment in the MGG8 model is mediated by effects other than vessel modulation.

A2V Treatment Promotes an Antitumor Macrophage Phenotype. Glioma-associated immune cell populations have the potential to create and maintain tumor progression and immunosuppression. To study the impact of antiangiogenic therapy on the tumor immune microenvironment, we analyzed cellular compartments of Gl261 tumors. First, we measured the presence and activation status of CD4$^+$ and CD8$^+$ T cells of Gl261 tumors treated for 10 d with IgG, B20, or A2V (Fig. S5). Next, we analyzed the presence and quantity of CD4$^+$ and CD8$^+$ T cells among lymphocytes and assessed their state of activation. In further analyses we measured the presence of the T-regulatory suppressive phenotype (Fig. S5) and the activation and proliferation state of CD4$^+$ and CD8$^+$ cells (Fig. S6). Our data indicate that treatment with B20 or A2V did not induce changes in the number, proliferation, or activation state in T-cell subsets within tumors. In further analyses, we measured the number and phenotype of TAMs. Our data indicate no significant changes in the presence of TAMs (as a percentage of total CD45$^+$ cells) among the treatment groups (Fig. 4). However, the percentage of M1-polarized antitumor TAMs (defined as CD206^{low}/CD11c^{high} and shown as a percentage

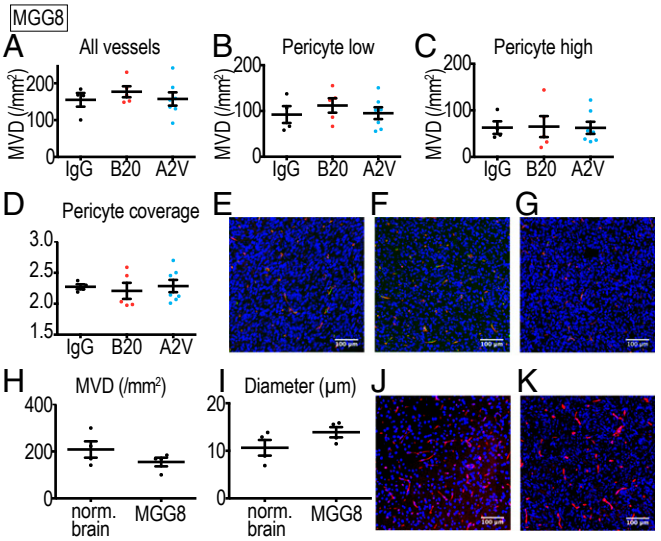

Fig. 3. Treatment with A2V and B20 had no vascular effects in the MGG8 model. (*A–D*) IgG, $n = 4$; B20 $n = 5$; A2V, $n = 7$. (*A*) No differences between treatment groups were detected in total MVD (vessels/mm^2) or in the MVD of vessels with low (*B*) or high (*C*) pericyte coverage. There were no differences in tumor vessel pericyte coverage (*D*). (*E–G*) Representative immunofluorescence images of IgG- (*E*), B20- (*F*), and A2V- (*G*) treated tumors. Shown are tumor vessels (red), pericytes (green), and DAPI-stained nuclei (blue). (*H*) No significant difference in MVD was seen between IgG-treated MGG8 tumors (at day 10 post treatment initiation, $n = 4$) and the normal brain (nl brain) of 10-wk-old mice ($n = 4$). (*I*) Mean vessel diameter in IgG-treated MGG8 tumor vessels ($n = 4$) is similar to that in the normal SCID brain ($n = 4$). (*J* and *K*) MGG8 vessels are homogeneously distributed throughout the tumor and display a regular shape, similar to normal brain vessels of SCID mice. Shown are representative immunofluorescence images of MGG8 tumor vessels stained for CD31 (red) and nuclei stained with DAPI (blue). MVD represents vessels/mm^2 tumor area; pericyte coverage represents desmin-positive pixels per vessel perimeter (pixels). (Scale bars, 100 µm.)

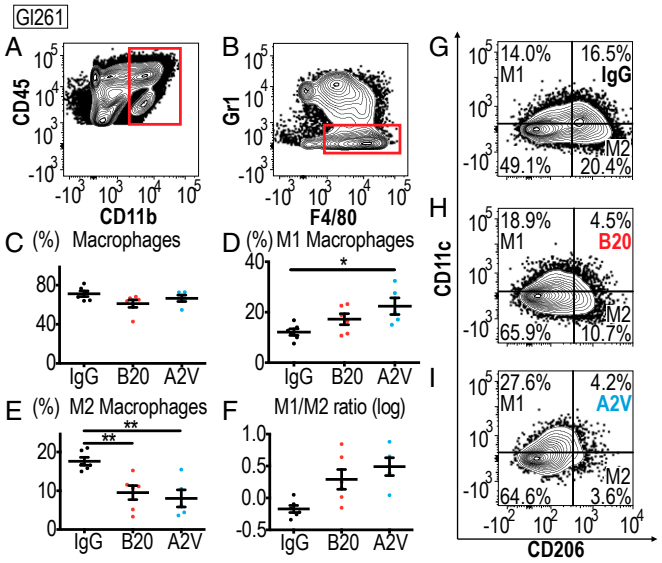

Fig. 4. In the Gl261 model treatment with A2V shifts TAMS toward the M1 state. In all panels, IgG, $n = 6$; B20, $n = 6$; A2V, $n = 5$. (*A* and *B*) Gating through CD45^{high}/CD11b^{+} and F4/80^{+}/GR1^{-} identified macrophages. (*C*) Treatment with A2V or B20 did not lead to significant changes in the total percentage (percent of all CD45^{pos} cells) of Gl261 tumor-infiltrating macrophages compared with IgG control. (*D*) The percentage of CD206^{low}/CD11c^{high} M1-polarized macrophages (as a percentage of total macrophages) was increased in A2V-treated Gl261 tumors as compared with IgG-treated tumors (*$P = 0.02$). (*E*) CD206^{high}/CD11c^{low} M2 macrophages were decreased by A2V treatment compared with IgG treatment (**$P = 0.004$). B20 therapy decreased M2 macrophages compared with IgG therapy (**$P = 0.01$). (*F*) The M1/M2 ratio showed a trend toward the M1 polarization state in A2V-treated animals compared with IgG-treated animals. (*G–I*) Representative gates for IgG (*G*), B20 (*H*), and A2V (*I*) to identify M1 and M2 macrophages.

of total macrophages) was significantly higher in A2V-treated tumors than in controls (Fig. 4 *D* and *G–I*). Moreover, the percentage of protumor M2 TAMs (defined as CD206^{high}/CD11c^{low}) was decreased by both B20 and A2V treatment (Fig. 4 *E* and *G–I*). The resulting ratio of M1/M2 TAMs was skewed toward the antitumor M1 phenotype (Fig. 4*F*). Within the total TAM population we distinguished between TAMs recruited from the blood circulation versus resident microglia populations. Our data indicate that changes in the overall TAM population were mediated chiefly by a phenotypic shift in recruited TAMs (Figs. S7 and S8). In agreement with these data, we found gene expression changes in TAMs suggestive of enhanced M1 (*Cxcl9*, *Il6*) and reduced M2 (*CD206*) polarization (Fig. S9). We observed no changes in the percentage of CD45^{+}/CD11b^{+}/GR1^{+} myeloid-derived suppressor cells (MDSCs) after treatment with B20 or A2V in the tumors (Fig. S10 *A–C*). Consistent with the data from the Gl261 model, flow cytometric analyses of MGG8 tumors after 10 d of treatment showed that therapy with IgG, B20, or A2V did not change the percentage of TAMs (Fig. 5). Moreover, A2V therapy and, to a lesser extent, B20 therapy also increased the percentage of M1 TAMs in MGG8 tumors as compared with IgG treatment (Fig. 5 *D* and *G–I*). Importantly, treatment with A2V reduced the percentage of protumor M2 macrophages as compared with IgG treatment. Treatment with B20 induced a similar reduction in M2 TAMs compared with IgG treatment (Fig. 5 *E* and *G–I*). The M1/M2 TAM ratio was significantly increased by A2V therapy (Fig. 5*F*). We observed significant reprogramming effects toward the M1 phenotype in both the recruited TAMs and the microglia after treatment with B20 and A2V (Figs. S11 and S12). As seen in the Gl261 model, MDSC infiltration was not affected by treatment with either B20 or A2V (Fig. S10 *C–E*).

Discussion

To date, targeting the VEGF pathway has failed to prolong overall survival in GBM patients (2, 6, 7, 9). We and others have shown previously that the elevation of Ang-2 levels may compromise the benefits of anti-VEGF therapy in preclinical GBM models (10, 14). Here, we tested whether dual inhibition of VEGF (with B20) and Ang-2 (with LC06) with a bispecific antibody (A2V) could improve therapy outcome over antiangiogenic monotherapy. Our study shows that A2V inhibits tumor growth and prolongs the survival of mice bearing syngeneic or human xenograft tumors as compared with anti–Ang-2 or VEGF therapy alone. These results are consistent with the effects of anti–Ang-2/VEGF therapy in extracranial tumor models (14, 27–30, 40). We further demonstrate in the Gl261 model that A2V prunes pericyte-low immature vessels, reducing microvascular density. In addition, A2V may reduce microvessel density by inhibiting EC sprouting. HUVEC sprouting was induced by rVEGF and by rAng-2, and sprouting was abrogated by the neutralization of both factors with A2V. Importantly, sprouting induced by rAng-2 plus rVEGF was inhibited by B20 and was completely abrogated by A2V but not by LC06 monotherapy. Surprisingly, B20-mediated neutralization of VEGF abrogated the sprouting induced by VEGF as well as that induced by Ang-2. The efficacy of B20 in reducing Ang-2–induced sprouting is in line with the codependent function of Ang-2 and VEGF in this angiogenic process (11, 14).

Although A2V delays tumor growth, it fails to achieve long-term inhibition of Gl261 tumor growth. Our data suggest that pericyte-high (mature) vessels are resistant to B20 and A2V therapy and therefore may support sustained tumor growth (39, 41, 42). These results are in line with the effects of VEGF

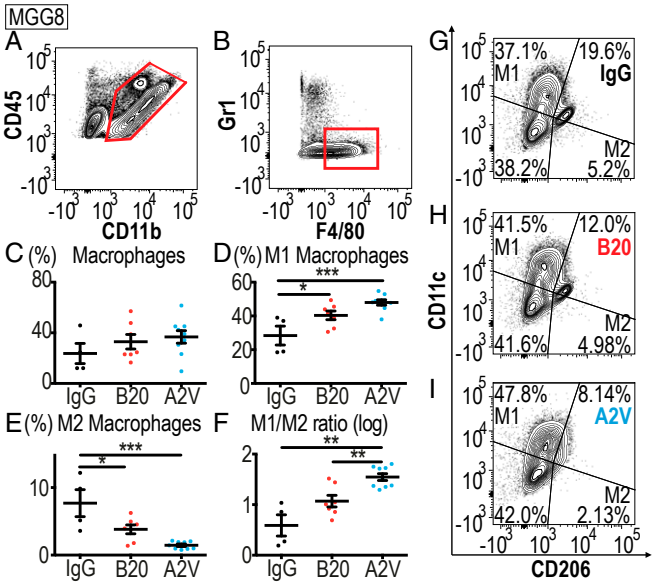

Fig. 5. Treatment with A2V increases MGG8-tumor associated M1 macrophages and reduces M2 macrophages. In all panels, IgG, $n = 4$; B20, $n = 7$; A2V, $n = 9$. (*A* and *B*) Gating through CD45^{high}/CD11b^{+} and F4/80^{+}/GR1^{-} identified macrophages. (*C*) Macrophage presence was not affected by treatment with B20 or A2V compared with IgG treatment. (*D*) The percentage of CD206^{low}/CD11c^{high} M1-positive macrophages (as a percentage of total macrophages) in A2V-treated tumors was increased compared with percentages in IgG-treated tumors (***$P < 0.001$). Treatment with B20 increased M1 macrophages compared with IgG treatment (*$P = 0.04$). (*E*) The percentages of CD206^{high}/CD11c^{low} M2 macrophages was reduced by A2V treatment compared with IgG (***$P < 0.001$). B20 reduced M2 macrophages as compared with IgG treatment (*$P = 0.02$). (*F*) The ratio of M1/M2 macrophages was skewed by A2V treatment toward the M1 phenotype as compared with IgG treatment (**$P = 0.002$) and B20 treatment (**$P = 0.008$). (*G–I*) Representative gates for IgG (*G*), B20 (*H*), and A2V (*I*) to identify M1 and M2 macrophages.

pathway inhibition described in preclinical tumors in our companion paper (43) and by others (42, 44), as well as our observations in breast cancer patients (45) that bevacizumab pruned vessels and normalized the remaining vasculature.

Many of the effects of dual anti–Ang-2/VEGF therapy—including the delay in tumor growth—were seen in a human GBM xenograft model (MGG8). In the MGG8 model, however, the benefits were more limited and occurred in the absence of any apparent antivascular effects. The differential vascular response to A2V in the Gl261 and the MGG8 models may be related to the structural differences in their vasculature; although Gl261 vessels are highly abnormal, MGG8 vessels are homogeneously distributed, and their architecture more closely resembles that of the normal mouse brain. Previously, it has been proposed that different blood vessel phenotypes exhibit differential susceptibility to anti-VEGF therapy (12, 46). Our results suggest that the tumor vessel phenotype also may be an important determinant of vascular response to dual anti–Ang-2/VEGF blockade, with immature vessels being most susceptible to therapy. Importantly, vascular phenotypes could be studied by imaging in GBM patients. For example, we demonstrated in clinical trials that vessel architectural imaging (VAI) could characterize the vascular phenotype and identify GBM patients who respond to anti-VEGF pathway inhibition (47, 48). Thus, VAI potentially may identify patients likely to benefit from the vascular component of dual anti–Ang-2/VEGF therapy.

In histological studies we detected no effects of either B20 or A2V on the rate of cancer cell apoptosis in either Gl261 or MGG8 tumors. This finding is confirmed further by the viability assays we conducted, showing no direct cytotoxic or cytostatic effects of A2V, and by data showing that the inhibition of the Tie2 pathway alone does not have cytotoxic effects in multiple tumor models (49). Indeed, neither Gl261 nor MGG8 express Tie2 (Fig. S4). However, A2V therapy reduced tumor cell proliferation as compared with B20 therapy both in Gl261 and MGG8 tumors, despite the differences in antivascular effects in these tumors.

Resident and infiltrating immune cells comprise a major component of the tumor microenvironment. Depending on the state of the disease or treatment, the immune compartment can either promote or inhibit tumor growth (50, 51). Among immune cells, the ability of T cells to eradicate tumor cells has been studied extensively (50). Treating tumors with mono (B20) or dual anti-angiogenic therapy (A2V) did not alter the presence of T cells or the specific functional T-cell phenotype (effector versus regulatory) in the tumors (Fig. S5). These $CD4^+$ and $CD8^+$ T cells were highly proliferative and were in an activated state regardless of the treatment (Fig. S6), suggesting that these T cells did not specifically differ in their exhaustion/anergy. It also should be noted that natural killer (NK) cells can impart antitumor functions independent of $CD8^+$ T-cell activation, although a previous report documented that NK cells have a lesser antitumor effect than $CD8^+$ T cells in Gl261 tumors (52). In addition, we studied TAMs as an abundant immune cell component in GBMs that may home to tumors in an Ang-2–dependent manner (15, 16) and promote tumor growth (18, 53, 54). Our finding that A2V treatment reprograms TAMs along the M1–M2 continuum toward the M1 phenotype in both Gl261 and MGG8 tumors may explain the survival benefit observed in these preclinical models, including the benefits seen with anti–Ang-2 monotherapy. This finding could have implications for the sequencing of potential combinatorial regimens of antiangiogenic agents with immunotherapy, because M1-polarized macrophages and microglia may hamper the efficacy of oncolytic herpes simplex virus-1 GBM therapy (55). The role of TAMs in GBM progression is highlighted further by the data presented in our companion paper (43), in which we demonstrate that TAM depletion with anti–CSF-1 antibody compromises the survival benefit of dual antiangiogenic therapy (Table S2).

Interestingly, reprogramming of the overall TAM population by A2V was largely attributable to recruited TAMs in Gl261 tumors and not to resident microglia. In contrast, we observed reprogramming of resident microglia-derived TAMs in the MGG8 tumors in SCID mice. The reprogramming may be caused by the large presence of microglia populations in SCID mice bearing MGG8 tumors as compared with C57BL mice bearing Gl261 tumors, in line with published data (56).

In summary, we show that dual Ang-2/VEGF blockade can increase the survival of mice bearing GBM over anti-VEGF therapy alone. This increased survival may be the result of the reprogramming of GBM-associated TAMs from the protumor M2 phenotype toward the antitumor M1 phenotype, as observed in both syngeneic murine tumors and human tumor xenografts. In GBMs with a high degree of vascular abnormality, this dual blockade approach also caused antivascular effects. These data support the development of anti–Ang-2/VEGF blockade for GBM alone or with immunotherapy (49, 57).

Materials and Methods

C57BL/6 mouse-syngeneic Gl261 cells (Frederick National Laboratory, National Cancer Institute) and human MGG8 GBM cells (58) were stereotactically implanted in the brains of male C57BL/6 mice and SCID mice, respectively. Tumor size was assessed by measuring circulating Gluc (35) activity in the blood. Treatment was initiated at a predefined Gluc blood activity (Fig. S3 *A* and *D*), and tumor burden was measured over time by serial blood Gluc measurements. Animals were treated with IgG, LC06 (Ang-2 antibody), B20 (VEGF antibody), or A2V (bispecific Ang-2/VEGF, CrossMab;) once weekly i.p. at 10 mg/kg. Brains were harvested at the described time points after injection of EdU and were paraffin embedded for histological analyses. The tissues were assessed for cell proliferation (EdU), microvessel density (CD31), and pericyte coverage (desmin). All animal procedures followed Public Health Service Policy on Humane Care of Laboratory Animals guidelines and were approved by the Massachusetts General Hospital Institutional Animal Care and Use Committee. The use of patient samples was approved by the internal review board of Massachusetts General Hospital. Experimental procedures and methods are described in detail in *SI Materials and Methods*.

ACKNOWLEDGMENTS. We thank T. J. Diefenbach and the Ragon Institute Imaging Core (Harvard Center for AIDS Research Immunology Core) for technical and instrumental support for microscopy; B. A. Tannous for technical support with the Gluc-GFP reporter system; M. Duquette, S. Roberge, P. Huang, A. Khachatryan, M. Tedy, O. Pulluqi, I. Gorr, S. Imhof-Jung, H. Dürr, T. v. Hirschheydt, M. Molhoj, H. Kettenberger, J. Moelleken, and H. Auer for outstanding technical assistance; and S. Chatterjee, M. Badeaux, S. Babykutty, T. Hato, D. Kodack, G. B. Ferraro, S. S. Islam, T. Mempel, T. Padera, Y. Huang, T. Peterson, S. M. Chin, S. Kozin, M. Thomas, K. Munro, M. Weidner, and H. J. Mueller for invaluable suggestions and experimental assistance. The study was supported in part by NIH Grants P50CA165962 (to T.T.B and R.K.J.), P01CA080124 (to R.K.J., D.G.D., D.F., and L.L.M.), KCA125440 (to T.T.B.), R01CA126642 and R35CA197743 (to R.K.J.), R01CA159258 (to D.G.D.), R01CA096915 (to D.F.), R01HL106584 (to L.L.M.), and S10-RR027070 (to D.F.); National Cancer Institute/Federal Share Proton Beam Program Income (R.K.J.); Department of Defense Breast Cancer Research Innovator Award W81XWH-10-1-0016 and National Foundation for Cancer Research Fellow Award (to R.K.J.); and a research grant from Hoffmann-La Roche. N.D.K. was supported by NIH Training Grant T32-CA073479. M.S., C.L.-E., and J.W.T. were supported by NIH Training Grant K12CA090354. J.K. received fellowships from the German Research Foundation (DFG) and the SolidarImmun Foundation. L.R. received a Mildred Scheel Fellowship (Deutsche Krebshilfe). Z.A. received a fellowship from the Aid for Cancer Research Foundation. G.S. was supported by Susan G. Komen Postdoctoral Fellowship PDF14301739. M.S. received research support from Affymetrix. V.A. received financial support from the DFG.

1. Stupp R, et al.; European Organisation for Research and Treatment of Cancer Brain Tumor and Radiotherapy Groups; National Cancer Institute of Canada Clinical Trials Group (2005) Radiotherapy plus concomitant and adjuvant temozolomide for glioblastoma. *N Engl J Med* 352(10):987–996.
2. Lu-Emerson C, et al. (2015) Lessons from anti-vascular endothelial growth factor and anti-vascular endothelial growth factor receptor trials in patients with glioblastoma. *J Clin Oncol* 33(10):1197–1213.
3. Cohen MH, Shen YL, Keegan P, Pazdur R (2009) FDA drug approval summary: Bevacizumab (Avastin) as treatment of recurrent glioblastoma multiforme. *Oncologist* 14(11):1131–1138.
4. Kreisl TN, et al. (2009) Phase II trial of single-agent bevacizumab followed by bevacizumab plus irinotecan at tumor progression in recurrent glioblastoma. *J Clin Oncol* 27(5):740–745.
5. Friedman HS, et al. (2009) Bevacizumab alone and in combination with irinotecan in recurrent glioblastoma. *J Clin Oncol* 27(28):4733–4740.
6. Gilbert MR, et al. (2014) A randomized trial of bevacizumab for newly diagnosed glioblastoma. *N Engl J Med* 370(8):699–708.
7. Chinot OL, et al. (2014) Bevacizumab plus radiotherapy-temozolomide for newly diagnosed glioblastoma. *N Engl J Med* 370(8):709–722.

8. Batchelor TT, et al. (2013) Phase III randomized trial comparing the efficacy of cediranib as monotherapy, and in combination with lomustine, versus lomustine alone in patients with recurrent glioblastoma. *J Clin Oncol* 31(26):3212–3218.
9. Wick W, et al. (2015) LB-05 * phase III trial exploring the combination of bevacizumab and lomustine in patients with first recurrence of a glioblastoma: The EORTC 26101 trial. *Neuro-oncol* 17(suppl 5):v1–v1.
10. Chae S-S, et al. (2010) Angiopoietin-2 interferes with anti-VEGFR2-induced vessel normalization and survival benefit in mice bearing gliomas. *Clin Cancer Res* 16(14): 3618–3627.
11. Maisonpierre PC, et al. (1997) Angiopoietin-2, a natural antagonist for Tie2 that disrupts in vivo angiogenesis. *Science* 277(5322):55–60.
12. Sitohy B, Nagy JA, Dvorak HF (2012) Anti-VEGF/VEGFR therapy for cancer: Reassessing the target. *Cancer Res* 72(8):1909–1914.
13. Augustin HG, Koh GY, Thurston G, Alitalo K (2009) Control of vascular morphogenesis and homeostasis through the angiopoietin-Tie system. *Nat Rev Mol Cell Biol* 10(3): 165–177.
14. Daly C, et al. (2013) Angiopoietin-2 functions as a Tie2 agonist in tumor models, where it limits the effects of VEGF inhibition. *Cancer Res* 73(1):108–118.
15. Venneri MA, et al. (2007) Identification of proangiogenic TIE2-expressing monocytes (TEMs) in human peripheral blood and cancer. *Blood* 109(12):5276–5285.
16. Gabrusiewicz K, et al. (2014) Anti-vascular endothelial growth factor therapy-induced glioma invasion is associated with accumulation of Tie2-expressing monocytes. *Oncotarget* 5(8):2208–2220.
17. Kostianovsky AM, Maier LM, Anderson RC, Bruce JN, Anderson DE (2008) Astrocytic regulation of human monocytic/microglial activation. *J Immunol* 181(8):5425–5432.
18. Li W, Graeber MB (2012) The molecular profile of microglia under the influence of glioma. *Neuro-oncol* 14(8):958–978.
19. Coffelt SB, et al. (2011) Angiopoietin 2 stimulates TIE2-expressing monocytes to suppress T cell activation and to promote regulatory T cell expansion. *J Immunol* 186(7):4183–4190.
20. De Palma M, et al. (2005) Tie2 identifies a hematopoietic lineage of proangiogenic monocytes required for tumor vessel formation and a mesenchymal population of pericyte progenitors. *Cancer Cell* 8(3):211–226.
21. Pucci F, et al. (2009) A distinguishing gene signature shared by tumor-infiltrating Tie2-expressing monocytes, blood "resident" monocytes, and embryonic macrophages suggests common functions and developmental relationships. *Blood* 114(4):901–914.
22. Coffelt SB, et al. (2010) Angiopoietin-2 regulates gene expression in TIE2-expressing monocytes and augments their inherent proangiogenic functions. *Cancer Res* 70(13): 5270–5280.
23. Sica A, Mantovani A (2012) Macrophage plasticity and polarization: In vivo veritas. *J Clin Invest* 122(3):787–795.
24. Noy R, Pollard JW (2014) Tumor-associated macrophages: From mechanisms to therapy. *Immunity* 41(1):49–61.
25. Mantovani A, Allavena P (2015) The interaction of anticancer therapies with tumor-associated macrophages. *J Exp Med* 212(4):435–445.
26. Lu-Emerson C, et al. (2013) Increase in tumor-associated macrophages after antiangiogenic therapy is associated with poor survival among patients with recurrent glioblastoma. *Neuro-oncol* 15(8):1079–1087.
27. Brown JL, et al. (2010) A human monoclonal anti-ANG2 antibody leads to broad antitumor activity in combination with VEGF inhibitors and chemotherapy agents in preclinical models. *Mol Cancer Ther* 9(1):145–156.
28. Kienast Y, et al. (2013) Ang-2-VEGF-A CrossMab, a novel bispecific human IgG1 antibody blocking VEGF-A and Ang-2 functions simultaneously, mediates potent antitumor, antiangiogenic, and antimetastatic efficacy. *Clin Cancer Res* 19(24):6730–6740.
29. Rigamonti N, et al. (2014) Role of angiopoietin-2 in adaptive tumor resistance to VEGF signaling blockade. *Cell Reports* 8(3):696–706.
30. Hashizume H, et al. (2010) Complementary actions of inhibitors of angiopoietin-2 and VEGF on tumor angiogenesis and growth. *Cancer Res* 70(6):2213–2223.
31. Hidalgo M, et al. (2014) Results from the first-in-human (FIH) phase I study of RO5520985 (RG7221), a novel bispecific human anti-ANG-2/anti-VEGF-A antibody, administered as an intravenous infusion to patients with advanced solid tumors. *ASCO Meeting Abstracts* 32(15_suppl):2525.
32. Murat A, et al. (2008) Stem cell-related "self-renewal" signature and high epidermal growth factor receptor expression associated with resistance to concomitant chemoradiotherapy in glioblastoma. *J Clin Oncol* 26(18):3015–3024.
33. Lambiv WL, et al. (2011) The Wnt inhibitory factor 1 (WIF1) is targeted in glioblastoma and has a tumor suppressing function potentially by induction of senescence. *Neuro-oncol* 13(7):736–747.
34. Barrett T, et al. (2013) NCBI GEO: Archive for functional genomics data sets–update. *Nucleic Acids Res* 41(Database issue):D991–D995.
35. Wurdinger T, et al. (2008) A secreted luciferase for ex vivo monitoring of in vivo processes. *Nat Methods* 5(2):171–173.
36. Tannous BA (2009) Gaussia luciferase reporter assay for monitoring biological processes in culture and in vivo. *Nat Protoc* 4(4):582–591.
37. Kodack DP, et al. (2012) Combined targeting of HER2 and VEGFR2 for effective treatment of HER2-amplified breast cancer brain metastases. *Proc Natl Acad Sci USA* 109(45):E3119–E3127.
38. Carmeliet P, Jain RK (2011) Principles and mechanisms of vessel normalization for cancer and other angiogenic diseases. *Nat Rev Drug Discov* 10(6):417–427.
39. Jain RK (2014) Antiangiogenesis strategies revisited: From starving tumors to alleviating hypoxia. *Cancer Cell* 26(5):605–622.
40. Keskin D, et al. (2015) Targeting vascular pericytes in hypoxic tumors increases lung metastasis via angiopoietin-2. *Cell Reports* 10(7):1066–1081.
41. Carmeliet P, Jain RK (2011) Molecular mechanisms and clinical applications of angiogenesis. *Nature* 473(7347):298–307.
42. Dvorak HF (2015) Tumor Stroma, Tumor Blood Vessels, and Antiangiogenesis Therapy. *Cancer J* 21(4):237–243.
43. Peterson TE, et al. (2016) Dual inhibition of Ang-2 and VEGF receptors normalizes tumor vasculature and prolongs survival in glioblastoma by altering macrophages. *Proc Natl Acad Sci USA* 113:4470–4475.
44. Dvorak HF, Nagy JA, Dvorak JT, Dvorak AM (1988) Identification and characterization of the blood vessels of solid tumors that are leaky to circulating macromolecules. *Am J Pathol* 133(1):95–109.
45. Tolaney SM, et al. (2015) Role of vascular density and normalization in response to neoadjuvant bevacizumab and chemotherapy in breast cancer patients. *Proc Natl Acad Sci USA* 112(46):14325–14330.
46. Benjamin LE, Golijanin D, Itin A, Pode D, Keshet E (1999) Selective ablation of immature blood vessels in established human tumors follows vascular endothelial growth factor withdrawal. *J Clin Invest* 103(2):159–165.
47. Emblem KE, et al. (2013) Vessel architectural imaging identifies cancer patient responders to anti-angiogenic therapy. *Nat Med* 19(9):1178–1183.
48. Emblem KE, et al. (2014) Vessel caliber–a potential MRI biomarker of tumour response in clinical trials. *Nat Rev Clin Oncol* 11(10):566–584.
49. Grenga I, Kwilas AR, Donahue RN, Farsaci B, Hodge JW (2015) Inhibition of the angiopoietin/Tie2 axis induces immunogenic modulation, which sensitizes human tumor cells to immune attack. *J Immunother Cancer* 3:52.
50. Gajewski TF, Schreiber H, Fu Y-X (2013) Innate and adaptive immune cells in the tumor microenvironment. *Nat Immunol* 14(10):1014–1022.
51. Quail DF, Joyce JA (2013) Microenvironmental regulation of tumor progression and metastasis. *Nat Med* 19(11):1423–1437.
52. Wu J, Waxman DJ (2015) Metronomic cyclophosphamide eradicates large implanted GL261 gliomas by activating antitumor Cd8(+) T-cell responses and immune memory. *OncoImmunology* 4(4):e1005521.
53. Wagner S, et al. (1999) Microglial/macrophage expression of interleukin 10 in human glioblastomas. *Int J Cancer* 82(1):12–16.
54. Zhai H, Heppner FL, Tsirka SE (2011) Microglia/macrophages promote glioma progression. *Glia* 59(3):472–485.
55. Meisen WH, et al. (2015) The impact of macrophage- and microglia-secreted TNFα on oncolytic HSV-1 therapy in the glioblastoma tumor microenvironment. *Clin Cancer Res* 21(14):3274–3285.
56. Lorke DE, Ip CW, Schumacher U (2008) Increased number of microglia in the brain of severe combined immunodeficient (SCID) mice. *Histochem Cell Biol* 130(4):693–697.
57. Ott PA, Hodi FS, Buchbinder EI (2015) Inhibition of immune checkpoints and vascular endothelial growth factor as combination therapy for metastatic melanoma: An overview of rationale, preclinical evidence, and initial clinical data. *Front Oncol* 5:202.
58. Wakimoto H, et al. (2009) Human glioblastoma-derived cancer stem cells: Establishment of invasive glioma models and treatment with oncolytic herpes simplex virus vectors. *Cancer Res* 69(8):3472–3481.
59. Yuan F, et al. (1994) Vascular permeability and microcirculation of gliomas and mammary carcinomas transplanted in rat and mouse cranial windows. *Cancer Res* 54(17):4564–4568.
60. Folkman J (1971) Tumor angiogenesis: Therapeutic implications. *N Engl J Med* 285(21):1182–1186.
61. Liang W-C, et al. (2006) Cross-species vascular endothelial growth factor (VEGF)-blocking antibodies completely inhibit the growth of human tumor xenografts and measure the contribution of stromal VEGF. *J Biol Chem* 281(2):951–961.
62. Thomas M, et al. (2013) A novel angiopoietin-2 selective fully human antibody with potent anti-tumoral and anti-angiogenic efficacy and superior side effect profile compared to Pan-Angiopoietin-1/-2 inhibitors. *PLoS One* 8(2):e54923.
63. Schaefer W, et al. (2011) Immunoglobulin domain crossover as a generic approach for the production of bispecific IgG antibodies. *Proc Natl Acad Sci USA* 108(27): 11187–11192.
64. Pace CN, Vajdos F, Fee L, Grimsley G, Gray T (1995) How to measure and predict the molar absorption coefficient of a protein. *Protein Sci* 4(11):2411–2423.
65. Song JW, Bazou D, Munn LL (2012) Anastomosis of endothelial sprouts forms new vessels in a tissue analogue of angiogenesis. *Integr Biol (Camb)* 4(8):857–862.
66. Duffy DC, McDonald JC, Schueller OJ, Whitesides GM (1998) Rapid prototyping of Microfluidic Systems in Poly(dimethylsiloxane). *Anal Chem* 70(23):4974–4984.
67. Song JW, Munn LL (2011) Fluid forces control endothelial sprouting. *Proc Natl Acad Sci USA* 108(37):15342–15347.